Passive Microwave Remote Sensing of Snow, Soil Moisture, Surface Temperature and Rain

Toshio Koike [1] and Hideyuki Fujii [2]

[1]Department of Civil Engineering, University of Tokyo Bunkyo-ku, Tokyo 113-8656, Japan Phone +81-(0)3-5841-6106, Fax +81-(0)3-5841-6130 E-mail: tkoike@hydra.t.u-tokyo.ac.jp

[2] Nagaoka University of Technology Nagaoka, 940-2188, Japan Phone/Fax: +81-258-47-9673 Email: fujii@hydro.nagaokaut.ac.jp

Land surface hydrological conditions have been considered to play an important role in the global and regional climate variability. Especially, snow, soil moisture, surface temperature, vegetation and rain are the key parameters which should be observed in the global scale. In this paper, new algorithms for these land surface hydrological parameters have been developed by introducing frequency and polarization dependencies of these parameters in the microwave radiative-transfer equations. The algorithms were applied to the TRMM Microwave Radiometer (TMI) and validated by using the ground data obtained in the Tibetan Plateau. The estimated snow, soil moisture, surface temperature, water content of vegetation and rain patterns corresponded reasonably to the observed ones.

Key Words : *passive microwave remote sensing, snow, soil moisture, surface temperature, vegetation, rain*

1. Introduction

Microwave remote sensing can directly measure the dielectric propaties which is strongly dependent on the liquid water content. The longer wave length is one of the advantages of microwaves. It is long enough to reduce the scattering effect of cloud particles and to makemicrowave sensors a useful all-weather sensor. The wave length in the microwave region has sensitivity to the scattering effect of snow grains and leaves. Microwave remote sensing has potential of the measurement of snow water equivalent and water content of vegetation. By using higher frequency channel, scattering effects of rain drops can also be detected. The independence of sun as a source of illumination is also one of the important reasons for using microwaves. We can obtain the data even in night. This advantage is more important in the case of non-sunsynchronous observation. In this study, new algorithms for snow, soil moisture, surface temperature and rain by using passive microwave sensors are developed based on microwave radiative transfer theory. They are applied to the satellite data form the TRMM Microwave Imager (TMI) and validated by using the ground data obtained in the Tibetan Plateau which has been suggested to play an important role in the variation of the Asian summer monsoon.

2. Algorithm bases

The microwave brightness temperature observed by satellites is expressed by the radiative transfer equa-

tion which consists of the land surface radiation attenuated by vegetation and precipitation fields, the radiation from vegetation attenuated by precipitation fields, and the radiation from precipitation fields.

In the snow algorithm, the relationship between the land surface radiation and snow water equivalent is obtained by a radiative-transfer theory based on a scattering dielectric layer over a homogeneous half-space (England, 1975). The total land surface brightness temperature is the sum of the direct component, the reflected sky radiation and the thermal radio emission from snowpack and soil, and the diffuse component, the radiation scattered from the direct field and diffuse field. Snow depth and physical temperature are estimated by inputting the observed brightness temperature at two different frequencies into a look-up table which is simulated based on the radiative transfer equation by assuming snow grain size and snow density and by neglecting the effects of vegetation and precipitation fields(Koike & Suhama, 1993).

In the soil moisture algorithm, vegetation is considered as an absorption and radiation layer on skin soil characterized by dielectric constant which depends on soil mositure. To incorporate the effects of surface roughness, the reflectivity is calculated by using a polarization-mixing parameter and a roughness parameter (Wang & Choudhury, 1981). Two indices, Soil Wetness Index (Koike et al., 1996) and Polarization Index (Paloscia & Pampaloni,1988), in which effects of physical temperature are removed, are introduced to estimate land surface soil moisture and water content of vegetation. A look-up table which shows the relationship between soil moisture, water content of vegetation and the two indices is calculated by the radiative transfer model. Soil temperature is estimated by inputting the estimated soil moisture and water content of vegetation into the radiative transfer model.

The precipitation algorithm is basically same as the soil moisture algorithm. Precipitation field is modeled as an scattering extinction layer over skin soil without vegetation cover. To make the algorithm simple, the effect of precipitation filed is taken account at higher frequency but not at lower one.

In this paper, TRMM TMI data is used for the above three algorithms. The snow algorithm is applied to the brightness temperature at 19GHz and 37GHz to estimate snow depth and snow physical temperature. For soil moisture, sensitivity is investigated by using several combinations of frequencies, 10GHz and 19GHz, 10GHz and 37GHz, and 19GHz and 37GHz. In the precipitation algorithm, 10GHz and 85GHz are used because the former has high sensitivity to soil moisture and the latter to precipitation. The three algorithms are applied to the TMI path data which is geo-corrected to latitude-longitude coordinate.

3. Validation data

The Tibetan Plateau has been suggested to play an important role in the variation of the Asian summer monsoon through its atmospheric heating processes. To understand the generation of the hottest air mass in the world over the Tibetan Plateau in summer, the land surface hydrological conditions and the precipitation should be observed in the plateau scale. The Intensive Observing Period (IOP) was implemented in 1998 for the purposes of establishing the satellite-based observing systems ansd clarifying the interactions between the land surface and the atmosphere over the Tibetan Plateau in the context of the Asian monsoon system by taking into account the importance of seasonal variations in key processes. The following measurement systems were deployed and operated continuously during the IOP: the 14 AWSs, PBL tower, two turbulent flux measurement systems, radio-sonde system, 7 barometers, 20 rain gauges, 3-D Doppler radar, snow particle measurement system, microwave radiometer, GPS receiver, 9 soil moisture and temperature measurement systems, and two river water level gauges.

4. Results of validation

The estimated snow physical temperature is in good agreement with the observed surface temperature by

using the infrared thermometer as shown in Figure 1, although the snow depth has not been validated because the lack of the ground-based snow depth data. The typical interannual variation pattern of spatial distribution of snow in the Tibetan Plateau was derived by applying the snow algorithm to the winter of 1997-1998 and 1998-1999.

Figure 2 shows that the estimated soil moisture corresponds reasonably to the soil moisture observed by the TDR sensor at 4cm in depth. Just after the heavy rainfall, the estimated soil moisture is larger than the observed at 4cm in depth because the TMI detected only surface where is much wetter than the deeper point. During dryer period, the algorithm provide underestimation because the surface dry up more rapidly the the deeper point. The monthly averaged diurnal cycle of the land surface physical temperature calculated by the proposed algorithm shows the same pattern of the observed one with several K bias as shown in Figure 3. The estimated water content of vegetation corresponds to the observed one by harvesting and drying the grass in the field in accuracy of 10% or less.

The patterns of estimated optical thickness of the precipitation field derived from the TMI corresponds to ones of spatial distributions of rain observed by the 3 Dimensional Doppler Radar as shown in Figure 4. The temporal variation of the optical thickness and soil moisture are in good correspondence to the spatially averaged ground-based rain data in the mesoscale experimental area and the TDR data at 4 cm in depth as shown in Figure 5 and 6, respectively. By checking the sampling time of the TMI, it is suggested that the estimation accuracy depends considerably on the relationship between the local rainfall occurrence patterns and the sampling time.

Acknowledgment

The data used in this paper was obtained by the GAME- Tibet project supported by the Ministry of Education, Science, Sport and Culture of Japan; the Science and Technology Agency of Japan; the National Space Development Agency of Japan; the Frontier Research System for Global Change; and the Chinese Academy of Science. This study is supported by the Core Research for Evolutional Science and Rechnology.

REFERENCES

1) England, A.W.: Thermal microwave emission from a scattering layer, J.Grophys.Res., 80(32), 4484-4496, 1975.
2) Koike,T. & Suhama T.: Passive-microwave remote sensing of snow, Annals of Glaciology, 18, 305-308, 1993.
3) Koike,T. et al.: Spatial and Seasonal Distribution of Surface Wetness Derived from Satellite Data , Proc. of the International Workshop on Macro-Scale Hydrological Modeling, 87-96, 1996.
4) Paloscia S. & Pampaloni P.: Microwave Polarization Index for Monitoring Vegetation Growth, Geosci. and Remote Sens., 26(5), 617-621, 1988.
5) Wang, J.R. & Choudhury, B.J.: Remote sensing of soil moisture content over bare fieldat 1.4GHz frequency, J.Geophys. Res., 86, pp5277-5282, 1981

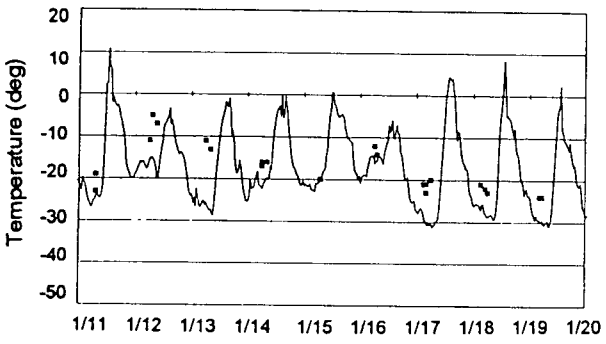

Figure 1 Time series of the estimaed snow physical temperature(plot) and observation(line)

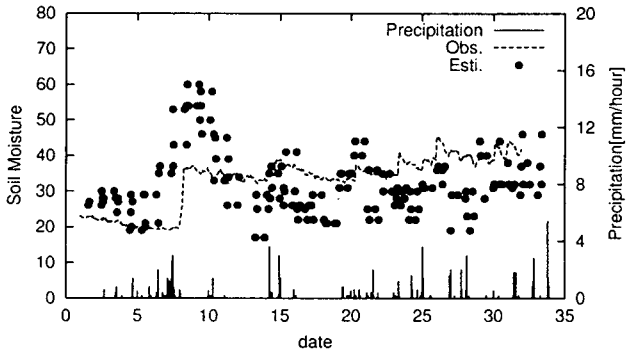

Figure 2 Time series of the soil moisture(July,1998)

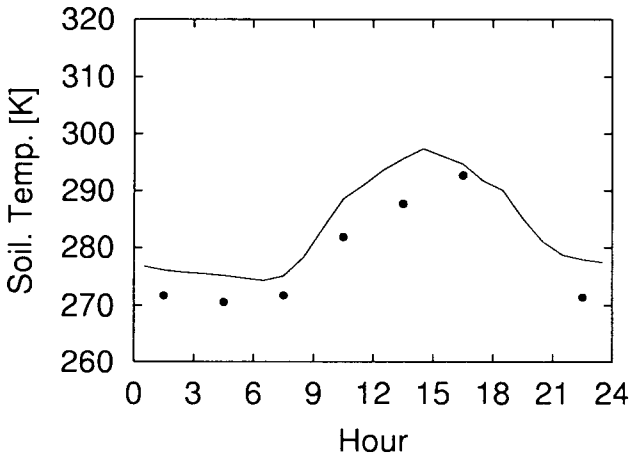

Figure 3 The monthly averaged diurnal cycle of the land surface physical temperature

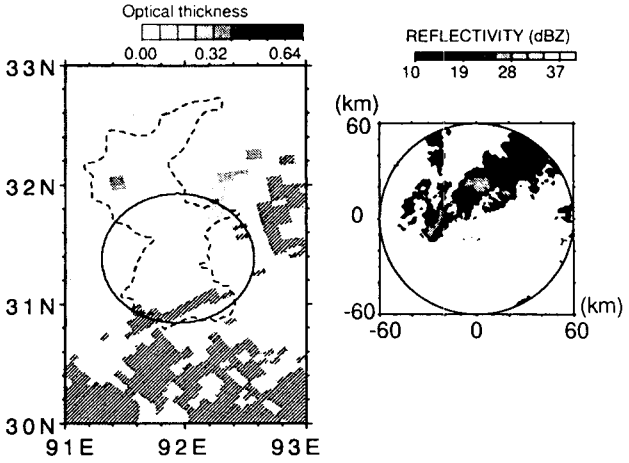

Figure 4 The optical thickness of the precipitation field(left) and PPI image observed by grand-based 3D radar(right)

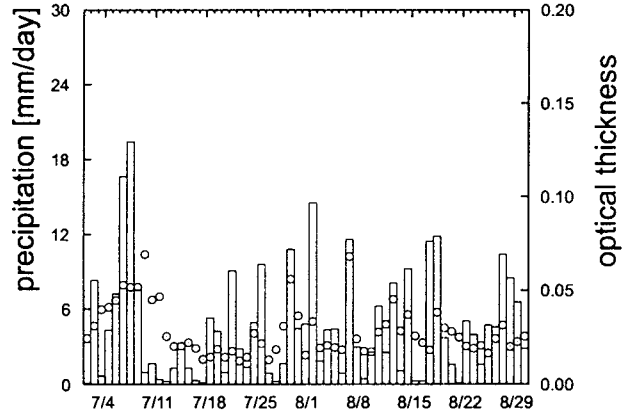

Figure 5 Time series of the estimated optical thickness(plot) and the observed rain data(bar)

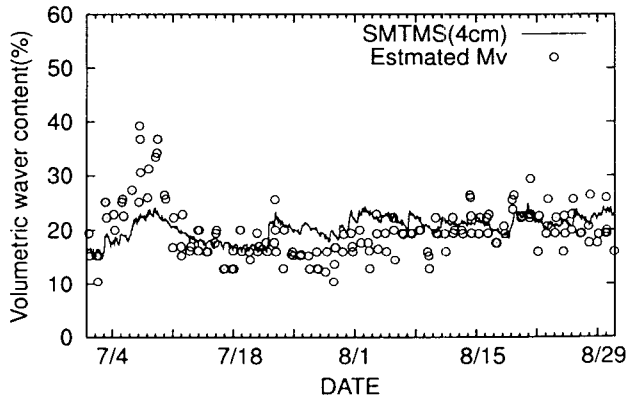

Figure 6 Time series of the estimated soil moisture(plot) and observation(line)